# Toward an Understanding of the Formation of Vanadia−Titania Catalysts

**Nisanth N. Nair, Thomas Bredow, and Karl Jug***

*Theoretische Chemie, Universität Hannover, Am Kleinen Felde 30, 30167 Hannover, Germany*

*Received: December 8, 2004; In Final Form: April 8, 2005*

Structures of hydrated vanadia species on the $TiO_2$-anatase surfaces were investigated using the semiempirical molecular orbital method MSINDO. The (101), (001), and (100) surfaces of anatase were considered. They were modeled by appropriate two-dimensional cyclic clusters of $TiO_2$. Monomeric and dimeric hydrated vanadia species on the anatase surfaces were simulated by adsorbing $VO_4H_3$ and $V_2O_7H_4$ molecules, respectively. Different adsorption structures were considered, and their stabilities at 300 and 600 K were tested by constant-temperature Born−Oppenheimer molecular dynamics simulations in the framework of MSINDO. Structural features of the vanadia−titania catalysts found in extended X-ray absorption fine structure, secondary ion mass spectrometry, IR, Raman, and NMR spectroscopy and conductivity experiments can be explained by the present calculations.

## 1. Introduction

Metal oxides have attracted much attention in the past two decades due to their wide range of applicability, especially in the field of heterogeneous catalysis.[1] Vanadia−titania ($V_2O_5$−$TiO_2$) catalysts are used in the selective catalytic reduction (SCR) of nitric oxides with ammonia.[2] In this process, nitric oxides produced in technical combustion processes are removed. Vanadia−titania catalysts are also employed for the partial oxidation of hydrocarbons.[3,4]

The most abundant crystalline states of titania are rutile and anatase. Rutile is thermodynamically stable, while anatase is metastable. It has been found that monolayer vanadia has a higher catalytic activity on anatase than on rutile in the SCR process. The observed increase of the catalytic activity has been attributed to the match between certain lattice planes of vanadia and anatase.[5]

Stable surfaces of anatase are the (101), (001), and (100) surfaces. Using periodic density functional theory (DFT) with local density (LDA) and generalized gradient (GGA) approximations, Lazzeri et al.[6] predicted that the anatase (101) surface is more stable than the other two surfaces. Beltran et al.[7] found that the anatase (001) surface is more stable than the (101) surface with B3LYP hybrid functional in the periodic DFT. The same conclusion was obtained in a study by Oliver et al.[8] based on classical interatomic potentials. The three surfaces have a different topology and can be expected to react differently with the vanadia particles.

Different preparative methods and reaction conditions are believed to affect the structure of the active vanadia species of the mixed catalyst.[9,10] The term "$VO_x$" is used for the active vanadia species on the surfaces of metal oxide supports. Various experimental techniques for the preparation and the investigation of the structure and catalytic properties of the vanadia−titania catalysts were reviewed.[9] IR and Raman spectroscopy probed the existence of isolated and polymeric vanadia species.[11] NMR studies helped to identify different vanadia species with varying vanadium coordination.[12] Extended X-ray adsorption fine structure (EXAFS) and X-ray adsorption near-edge structure (XANES) investigations detected novel vanadia species, for example, with divanadyl groups.[13] Experimental techniques were also used for the understanding of the reactivity of this catalyst.[10] The effects of hydration and preparative methods on the structure of the catalyst were also experimentally investigated.[14]

But to obtain a detailed picture of the structure of the catalyst on the atomic scale, theoretical investigations are necessary. Sayle et al.[15] studied the structure of vanadia multilayers on the anatase (001) surface using classical potentials. Interfaces formed by the interaction of different lattice planes of $V_2O_5$ with the anatase (001) surface were investigated. Significant deformations were found in the structure of $V_2O_5$ layers on the anatase (001) surface. Ferreira and Volpe[16] used extended Hückel calculations to predict the structures of different vanadia species on different oxide surfaces. A vanadia−titania catalyst was modeled by the adsorption of a $V_2O_5$ molecule on the anatase (100) and (001) surfaces by Calatayud et al.[17] Bredow et al.[18] proposed a model where a $V_2O_7H_4$ entity was adsorbed on the anatase (100) surface. It was based on experimental observations of polyvanadate chains with $VO_4$ units at low vanadia concentrations. Adsorption studies of NO, $NH_3$, and $H_2O$ were performed.[19] The same model was used to investigate the reaction mechanism of SCR of NO with $NH_3$ on anatase.[20] Calatayud and Minot[21] have studied the reactivity of the different oxygen sites in a model of $V_2O_5$ supported on anatase by periodic DFT calculations. They found that the most reactive sites are located at the interface between the $V_2O_5$ and the $TiO_2$ units. Vittadini and Selloni[22] also performed periodic DFT calculations on vanadia−titania catalysts. They have studied thermodynamic stabilities of vanadia species at various coverages on the hydrated (001) anatase surface. In their most recent work, they studied the mechanism of NO selective reduction on such vanadia−titania catalysts. Their model comprises only a fraction of the 24 steps that we proposed.[20] Despite their claim of higher numerical accuracy, no significant new insight was gained.

In previous studies on the stability of vanadia species, only static approaches were used. In the present work, molecular dynamics (MD) techniques were employed to study the reaction of hydrated vanadia species with the (101), (001), and (100)

* Author to whom correspondence should be addressed. E-mail: Jugthc@mbox.theochem.uni-hannover.de.

10.1021/jp044424h CCC: $30.25 
Published on Web 06/01/2005

anatase surfaces. Stabilities of different isolated and polymeric vanadia species were investigated. The main focus of this work is on the influence of various types of anatase surfaces on the structure of vanadia species.

## 2. Computational Details

MSINDO[24] is a modified version of the semiempirical self-consistent field (SCF) molecular orbital method SINDO1.[25] MSINDO uses a pseudominimal basis set and takes into account the core electrons by Zerner's local pseudopotential.[27] MSINDO has been parametrized for the elements H, Li−F, Na−Cl, and K−Br.[28−30] The parameter set used for Ti, V, O, and H in the present calculations is listed in this work.[30] With these parameters, MSINDO has been successfully applied to the study of vanadium pentoxide and titanium dioxide[31] and subsequently to adsorption and catalytic processes on anatase[20] and mixed vanadia−titania[18,19] surfaces.

For the description of solid bulk and surfaces, the cyclic cluster model (CCM) has been incorporated in MSINDO.[32] In the CCM, periodicity of the finite cluster is achieved by appropriate translations of the cluster atoms. In this way, every local part of the cluster that is translationally equivalent will have the same environment, and the local symmetry is preserved throughout the cluster. This is best understood as a topological concept of a cyclic arrangement.[33] Long-range electrostatic interactions can be approximately taken into account in CCM calculations by embedding in point charges. Interaction between the point charges and the atoms of the cyclic cluster is calculated using the Ewald summation technique.[31]

Recently Born−Oppenheimer MD has been implemented in MSINDO.[34] As electronic structural calculations using MSINDO are computationally faster than with other high-level methods, MD in conjunction with MSINDO can be used to generate classical trajectories of large and complex systems for time scales of several picoseconds. Equations of motion are integrated using the velocity Verlet algorithm.[35] A time step of 1 fs was used in the simulations. Constant-temperature MD simulations were performed using the Nosé−Hoover chain (NHC) thermostat.[36] In experiments, a wide range of temperatures has been used from room temperature up to 1000 K. As a standard reference temperature, we have chosen 300 K for our MD simulations. Olthof et al.[37] have done Raman measurements at room temperature (298 K). Calcination of the catalyst at temperatures above 600 K is usually performed after its preparation, mainly for dehydrating the catalyst. In our calculations, we have only considered dehydrated surfaces. Dehydration starts at 470 K.[10] The stability of the structures obtained from the MD simulations at 300 K has been further tested by separate constant-temperature MD simulations at 600 K. The temperature and the time scale used in the present calculations cannot take into account structural changes due to processes such as diffusion of surface atoms and reconstruction of the anatase surface.

## 3. Models

$VO_x$−$TiO_2$ catalysts are modeled by the adsorption of $VO_4H_3$ and $V_2O_7H_4$ on the anatase (101), (001), and (100) clean surfaces. $VO_4H_3$ and $V_2O_7H_4$ are the simplest realistic models to understand the structures of the $VO_x$−$TiO_2$ catalysts. In $VO_4H_3$, vanadium is tetrahedrally coordinated. In many of the preparative methods, the starting materials contain vanadium in tetrahedral coordination.[9,10] If water is present, then the vanadium species will be hydrated. For example, $VOCl_3$ can react with water initially present on the anatase surface to form $VO_4H_3$. Different types of hydrated species are possible depending on the pH of the medium.[14] Hydration is also possible by atmospheric water and from water molecules adsorbed on titanium dioxide.[12,14] There is experimental evidence for the presence of a hydrated $VO_x$ species on the $TiO_2$ support.[12,38,39] Ferreira and Volpe[16] have also used $VO_4H_3$ as a model in their simulations. The measurements after calcination were then on the dehydrated anatase surfaces.

**TABLE 1: Anatase Lattice Parameters *a* and *c* (Å) and Oxygen Fractional Coordinate *u***

| method | a | c | u |
|---|---|---|---|
| MSINDO | 3.630 | 9.783 | 0.205 |
| DFT[a] | 3.735 | 9.534 | 0.203 |
| experiment[b] | 3.786 | 9.514 | 0.208 |

[a] Reference 7. [b] Reference 40.

The MSINDO CCM three-dimensional (3D) calculation for bulk anatase simulation was performed using a $Ti_{64}O_{128}$ cluster. In a previous study,[31] this cluster was found to give converged bulk properties for a CCM-3D calculation. With this cluster, the anatase unit cell parameters were calculated. The optimized lattice parameters were $a = 3.630$ Å, $c = 9.783$ Å, and the oxygen fractional coordinate $u = 0.205$ (Table 1). They were in reasonable agreement with the values reported from a previous DFT calculation ($a = 3.735$ Å, $c = 9.534$ Å, and $u = 0.203$)[7] and experiment ($a = 3.786$ Å, $c = 9.514$ Å, and $u = 0.208$).[40] Surfaces energies were also calculated. Two-dimensional (2D) cyclic clusters $Ti_{96}O_{192}$ ($1 \times 3 \times 1$), $Ti_{108}O_{216}$ ($1 \times 3 \times 3$), and $Ti_{72}O_{144}$ ($1 \times 3 \times 6$) were used for modeling the (101), (001), and (100) surfaces, respectively. Bulk positions of all atoms in nine, nine, and five atomic layers, respectively, on both sides of the three clusters were relaxed during geometry optimization. The calculated surfaces energies were 1.31 J/m$^2$ for (101), 1.36 J/m$^2$ for (001), and 1.51 J/m$^2$ for (100) surfaces. Thus, the stability of the surfaces increases in the order (100) < (001) < (101). Lazzeri et al.[6] reported that the order of increasing stability is (001) < (100) < (101), while Beltran et al.[7] via DFT/B3LYP calculations and Oliver et al.[8] via simulations with classical potentials arrived at the stability sequence (100) < (101) < (001). We agree with Lazzeri et al. that the (101) surface is the most stable one. This was also observed in experiments.[41] There, a stable ($1 \times 1$) unreconstructed surface was found.

In the present work, three different $Ti_{36}O_{72}$ clusters were used for modeling the (101), (001), and (100) anatase surfaces by CCM-2D calculations. These clusters are shown in Figure 1. The optimized anatase−bulk lattice parameters were used for these clusters. Only a few top layers of each cluster were relaxed during the simulations. For the (101) and (001) clusters, the first six atomic layers and for the (100) cluster the first three atomic layers were relaxed. The cluster used to simulate the (101) surface does not have a complete repeating unit in the [101] direction. The (101) cluster with a complete unit cell along *z* direction has the size $Ti_{96}O_{192}$. To avoid excessive computer time in MD simulations, the smaller cluster $Ti_{36}O_{72}$ was chosen, which contains the basic structural features of the $Ti_{96}O_{192}$ cluster. But it was found that the error due to the use of the smaller $Ti_{36}O_{72}$ cluster instead of $Ti_{96}O_{192}$ was dispensable. For example, the calculated adsorption energies for molecular adsorption of a water molecule on $Ti_{36}O_{72}$ and $Ti_{96}O_{192}$ clusters were −99 and −95 kJ/mol, respectively.

In the present work, we have only considered the dehydrated anatase surfaces. The effect of the hydrated surface on the structure of the vanadia catalyst will be discussed in a forthcoming paper.[42]

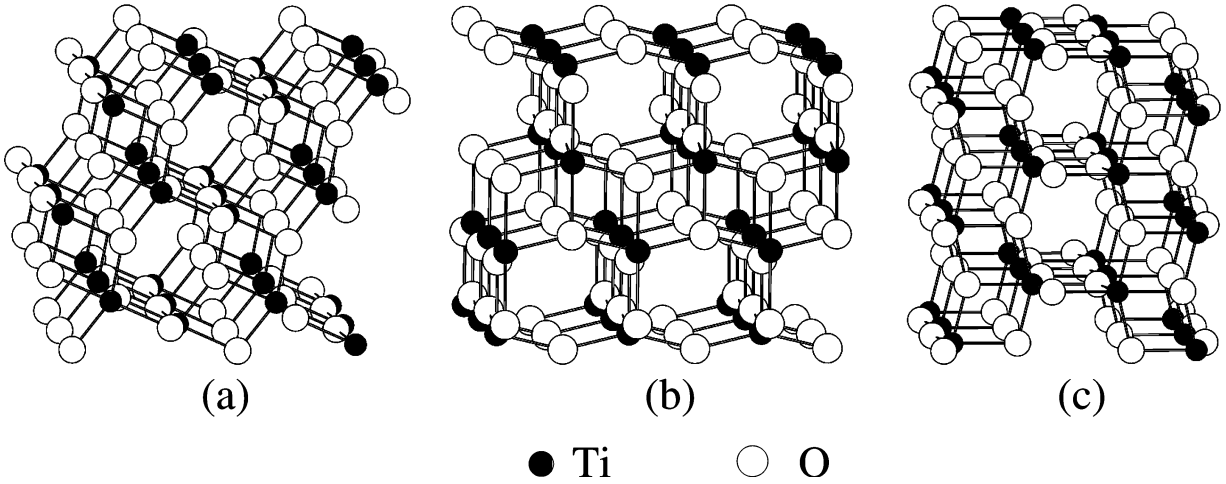


**Figure 1.** $TiO_2$ clusters ($Ti_{36}O_{72}$) used for modeling of $VO_x-TiO_2$ catalysts: (a) anatase (101), (b) anatase (001), (c) anatase (100).

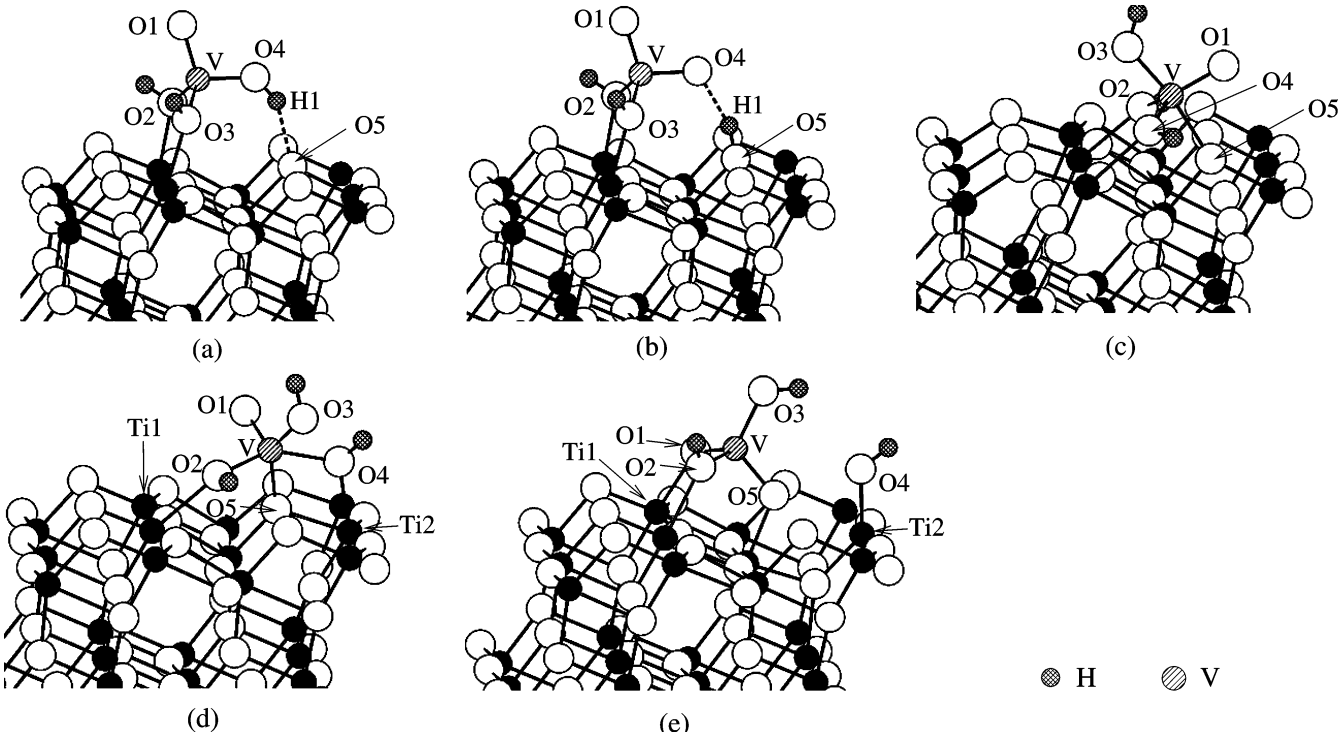


**Figure 2.** Different structures of $VO_4H_3$ on the anatase (101) surface. The dotted lines indicate hydrogen bonds; see also Figure 1 for types of atoms.

## 4. Results and Discussion

**4.1. Adsorption of $VO_4H_3$ on Anatase Surfaces.** *4.1.1. Anatase (101).* In a first step, $VO_4H_3$ was molecularly adsorbed on the anatase (101) surface. An adsorption structure shown in Figure 2a was considered first. In this structure, two oxygen atoms of $VO_4H_3$ are bound to two neighboring 5-fold coordinated surface titanium atoms. The hydrogen atom H(1) of $VO_4H_3$ is connected to the bridging surface oxygen O(5) by a hydrogen bond. The adsorption energy for this structure is −125 kJ/mol. The energy of the system further decreases by 25 kJ/mol, if the proton moves to the bridging surface oxygen atom O(5) (Figure 2b). The optimized lengths of all vanadium−oxygen bonds in the adsorbate structure are given in Table 2. The bond lengths of two vanadyl bonds V−O(4) and V−O(1) in the structure (Figure 2b) are 1.61 and 1.60 Å, respectively. The former bond is slightly longer because it is involved in a hydrogen bond to H(1).

**TABLE 2: Adsorption Energies $E_{ads}$ (kJ/mol) and Vanadium−Oxygen Bond Lengths (Å) of Different Adsorbed $VO_4H_3$ Structures on the Anatase (101), (001), and (100) Surfaces**

| | | | bond length | | | | |
|---|---|---|---|---|---|---|---|
| surface | structure | $E_{ads}$ | V−O1 | V−O2 | V−O3 | V−O4 | V−O5 |
| (101) | Figure 2a | −125 | 1.58 | 1.76 | 1.77 | 1.71 | |
| | Figure 2b | −150 | 1.60 | 1.83 | 1.84 | 1.61 | |
| | Figure 2c | −146 | 1.59 | 1.81 | 1.74 | 1.81 | |
| | Figure 2d | −155 | 1.59 | 1.82 | 1.76 | 1.93 | 1.81 |
| | Figure 2e | −208 | 1.64 | 1.79 | 1.73 | | 1.65 |
| (001) | Figure 5a | −294 | 1.60 | 1.80 | 1.86 | 1.84 | 1.79 |
| | Figure 5b | −450 | 1.59 | 1.82 | 1.94 | 1.83 | 1.73 |
| (100) | Figure 7a | −231 | 1.59 | 1.81 | 1.81 | 1.77 | 1.88 |

Two other adsorption structures were tested in which the vanadium atom is directly bound to the bridging oxygen O(5) (Figures 2c and 2d). The structure in Figure 2c is 4 kJ/mol higher

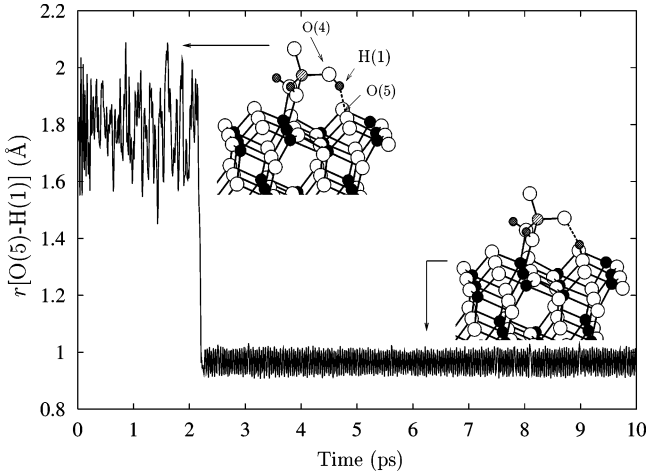


**Figure 3.** Distance $r$[O(5)−H(1)] (Å) between the oxygen O(5) and hydrogen H(1) during the MD simulation at 300 K. See Figures 1 and 2 for types of atoms.

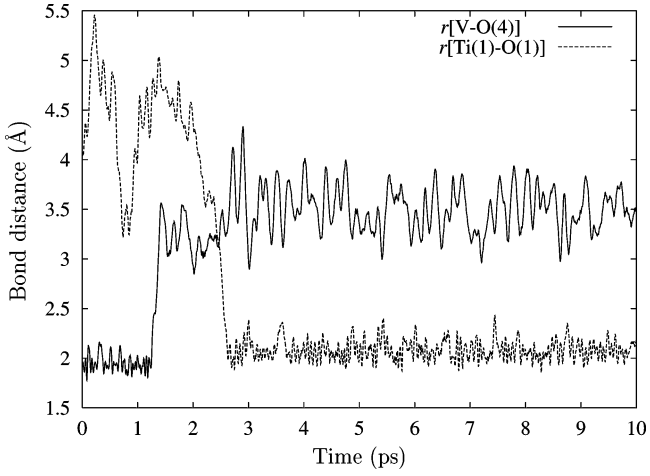


**Figure 4.** Distances $r$[V−O(4)] and $r$[Ti(1)−O(1)] (Å) during the MD simulation at 600 K for the structure in Figure 2d. See Figure 2d for labeling.

in energy than the structure in Figure 2b. The structure in Figure 2d turned out to be the most stable among all the structures in Figure 2. This structure is 5 kJ/mol more stable than the dissociated structure in Figure 2b. Vanadium is 5-fold coordinated, and the $VO_4$ tetrahedron of the $VO_4H_3$ molecule is distorted in this structure. The adsorbate partially forms a continuation of the crystal surface. Optimized bond lengths of all vanadium−oxygen bonds present in these two structures are given in Table 2.

To investigate the stability of these structures at high temperatures, constant-temperature MD simulations were performed at 300 K for 10 ps. The NHC thermostat was used for controlling the temperature during these simulations. The frequency of the thermostat was set to 3600 $cm^{-1}$, which is close to the maximum frequency of vibration of the system. The same procedure was used for all constant-temperature MD simulations presented in this section. The optimized structure in Figure 2a was used as starting point for the MD simulation. Within 2.2 ps, the O(4)−H(1) bond was broken, and the hydrogen was transferred to the bridging surface atom O(5). The structure in Figure 2a must therefore be considered as only metastable with respect to the structure in Figure 2b. The distance between the bridging oxygen and the proton of the adsorbate ($r$[O(5)−H(1)]) during this MD simulation is shown in Figure 3. The dissociated structure remained stable during the rest of the simulation for 10 ps. But no transformation from the structure in Figure 2b to the structure in Figure 2d was observed. Another MD simulation for 10 ps at 300 K was performed starting with the structure in Figure 2d. No remarkable structural rearrangements occurred during this simulation. As a conclusion, both of the structures in Figures 2b and 2d are stable at room temperature and may coexist.

For the study of the stability of the structures in Figures 2b and 2d at 600 K, MD simulations were performed at this temperature starting with these structures obtained at 300 K. Within 10 ps, no structural changes were observed for the structure in Figure 2b. But in the structure in Figure 2d, the V−O(4) bond (Figure 4) was dissociated after 1.4 ps, and a surface hydroxyl group was formed on Ti(2). After about 2.6 ps, the O(1) atom had moved toward the surface plane, and a bond with Ti(1) was formed (Figure 4), resulting in a tetrahedral arrangement at the V atom (Figure 2e). This structure remained stable during the rest of the simulation. The structure in Figure 2e is 53 kJ/mol more stable than the structure in Figure 2d. The adsorption energy and V−O bond lengths are given in Table 2.

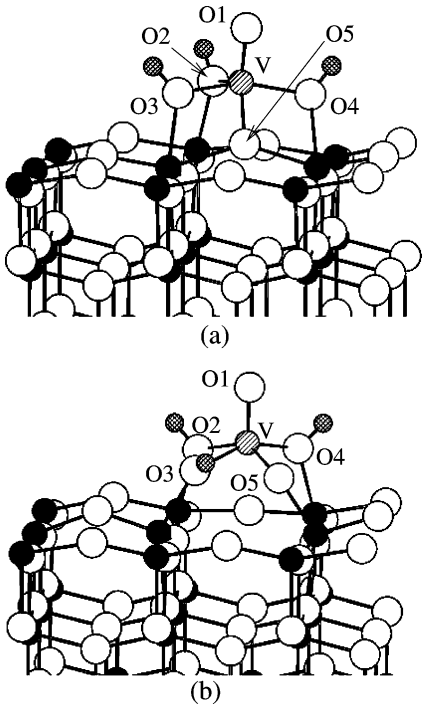


**Figure 5.** Different structures of $VO_4H_3$ on the anatase (001) surface. See Figures 1 and 2 for types of atoms.

*4.1.2. Anatase (001).* On the anatase (001) surface, three oxygen atoms of $VO_4H_3$ can bind to three five-coordinate surface titanium atoms as shown in Figure 5a. The $VO_4$ tetrahedron is distorted by the adsorption due to the interaction with the surface, and a bond between the vanadium atom and the surface oxygen O(5) is formed. The adsorption energy is −294 kJ/mol.

A MD simulation was performed at 300 K starting from the structure in Figure 5a. After a few steps of the simulation, the 2-fold coordinated surface oxygen O(5) to which the vanadium atom was connected moved out from its lattice position, and the structure in Figure 5b was formed. The displacement $\Delta r$ of the oxygen atom O(5) from its lattice position during the simulation process is shown in Figure 6. The oxygen atom moved by 1.3−1.5 Å from its lattice position during the dynamics simulation. The final structure in Figure 5b is about 156 kJ/mol more stable than the structure in Figure 5a. The V═O(1) and V−O(4) bond lengths slightly decreased by 0.01

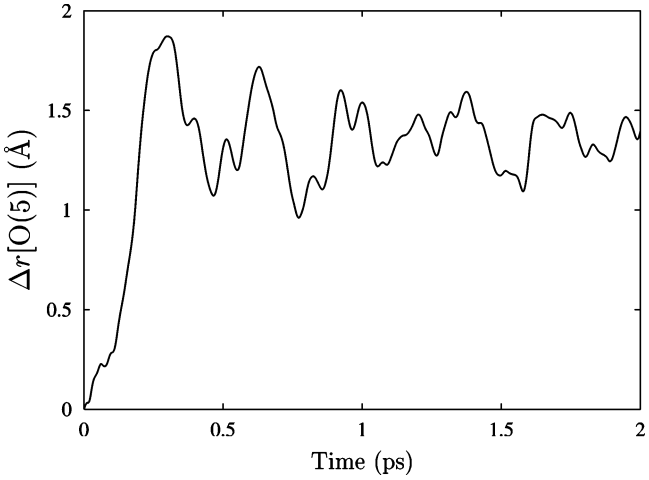


**Figure 6.** Displacement Δ*r* (Å) from the regular lattice position of the surface oxygen O(5), which is bound to the vanadium atom. See Figure 4 for the labeling of atoms.

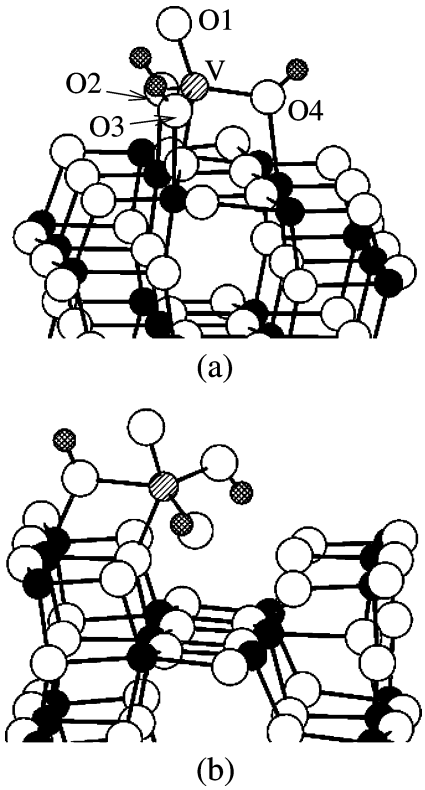


**Figure 7.** Different structures of $VO_4H_3$ on the anatase (100) surface. See Figures 1 and 2 for types of atoms.

Å, and the V−O(5) bond decreased from 1.79 to 1.73 Å. In contrast, the bond lengths of the other two V−O bonds increased (Table 2). No further change in the structure was observed during the rest of the MD simulation for 10 ps. In a separate MD simulation at 600 K, no structural rearrangements occurred in the structure in Figure 5b. This shows that the structure in Figure 5b is stable.

*4.1.3. Anatase (100).* On the anatase (100) surface, three oxygen atoms of $VO_4H_3$ can bind to three 5-fold coordinated titanium atoms on the surface without significant distortion of the tetrahedral structure (Figure 7a). In the optimized structure, the vanadyl V−O(1) bond is slightly tilted by about 20° from the surface normal. The vanadium atom is bound to one of the 3-fold coordinated surface oxygens. This oxygen atom O(5) is slightly displaced out of the surface. The V−O(1) bond length is 1.59 Å; the vanadium-to-surface oxygen bond length V−O(5) is 1.88 Å (Table 2).

The anatase (100) surface has channels along the [010] direction. In another structure, $VO_4H_3$ was adsorbed in such a way that the vanadium atom is directly connected to one of the 2-fold coordinated oxygens exposed at the edges of the channel (Figure 7b). This structure is found to be 104 kJ/mol higher in energy than the structure in Figure 7a.

MD simulations at 300 and 600 K were performed by starting with the energy minimum structure (Figure 7a) for 10 ps. This structure did not undergo any significant changes during these simulations and is therefore stable.

*4.1.4. Discussion.* Different types of bonding environments are present on the three different surfaces of anatase. The topology of the surface determines the structure of the vanadia species after adsorption. In most of the stable structures formed by the adsorption of $VO_4H_3$ on the three anatase surfaces, vanadium atoms are 5-fold coordinated. Using UV−vis−near-IR spectroscopy, Larrubia and Busca[43] reported that vanadium in vanadium oxide species on the supported catalysts has lower coordination than in bulk vanadia, being possibly four- or five-coordinated.

On the anatase (101) surface, a tetrahedral $VO_4$ environment is possible, as shown in Figures 2b and 2e. Even though the adsorption shown in Figure 2e is the most stable one, the structures in Figures 2b and 2e might coexist under experimental conditions. On the basis of an EXAFS/XANES analyses, Kozlowski et al.[13] predicted a structure similar to that in Figure 2b. In a secondary ion mass spectrometry (SIMS) experiment, Bond et al.[44] observed ions of type $V_xO_yH^+$. These were believed to originate from a species containing VO(OH) groups. The authors used a structure similar to that in Figure 2a as the basis of their interpretation. But the structure in Figure 2e can also be the source for producing $VO_yH^+$ ions. It is interesting to note that the tetrahedral arrangement in Figure 2e contains a vanadium bond with a surface oxygen but no V=O bond.

A distorted square-pyramidal type of structure was found for the monomeric vanadia species on the anatase (001) surface. The formation of a $VO_5H_3$ species is connected with the formation of an oxygen vacancy on the anatase surface. A similar bonding situation with square-pyramidal $VO_5$ units exists in the vanadium pentoxide (001) surface. The observed decrease in energy due to this rearrangement might be due to the formation of a less strained structure. Direct experimental evidence for the structure on the (001) surface could not be found in the literature. But there are some experimental observations that can be connected to the findings of this work. By electrical conductivity measurements, Herrmann[45] found that the concentration of anionic vacancies in the $TiO_2$ support increases with increasing vanadia loading. This might be due to the interaction of the surface oxygen with the adsorbate as discussed in section 4.1.2. Moreover, Went et al.[46] predicted $VO_x$ species of the O=$VO_4$ type in square-pyramidal structures on the anatase (001) surface. This interpretation was based on the data obtained from in situ laser Raman[46,47] and NMR spectroscopy[48] experiments. This supports the structure in Figure 5b. On comparison of the adsorption energies of $VO_4H_3$ on the three surfaces, it is clear that adsorption is more favorable on the anatase (001) surface than on the (100) or the (101) surfaces.

The tetrahedral structure of the adsorbate is almost preserved on the (100) surface. In most spectroscopic analyses of the $VO_x$−$TiO_2$ catalysts, there is clear evidence that the monomeric $VO_x$ species has tetrahedral coordination. Many experimental

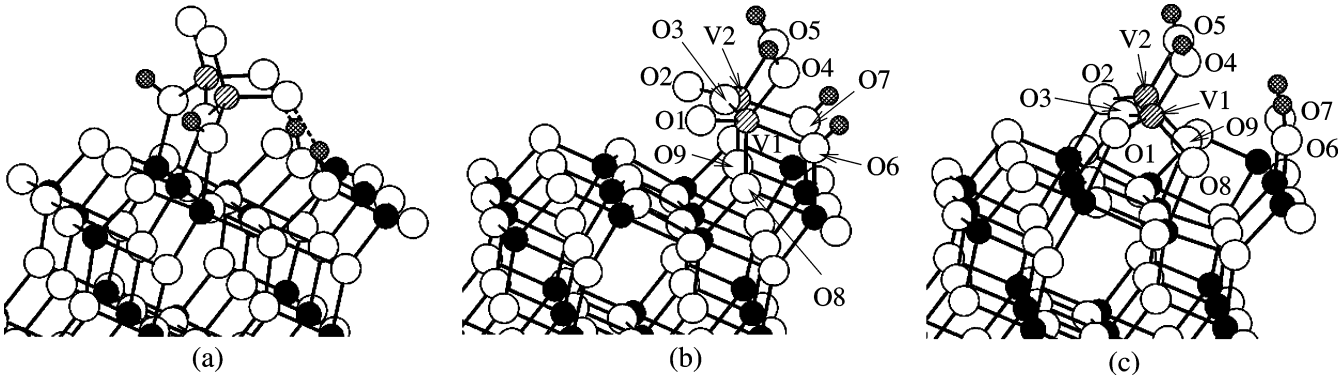


**Figure 8.** Different structures of $V_2O_7H_4$ on the anatase (101) surface. See Figures 1 and 2 for types of atoms.

investigations confirmed the existence of $VO_4$ tetrahedra, with three oxygens connected to the surface titanium atoms.[11,43,49−51] They assumed a structure similar to the one observed on the anatase (100) surface (Figure 7).

There are a few experimental data on bond lengths. From EXAFS measurements,[13] two ranges of vanadium−oxygen bond lengths were deduced: 1.60−1.70 Å for V═O and 1.85−1.95 Å for V−O. Our present calculations are in agreement with these.

**4.2. Adsorption of $V_2O_7H_4$ on Anatase Surfaces.** In this section, the results of the $V_2O_7H_4$ adsorption on the three anatase surfaces are presented. Several experimental studies reported the formation of polyvanadates on the $TiO_2$ surface at higher vanadia concentrations.[9] Polyvanadates can be formed before reaching the surface or by condensation reactions on the surface. It was assumed that the following reaction occurred between two $VO_4H_3$ molecules before or after adsorption.

$$2VO_4H_3 \rightarrow V_2O_7H_4 + H_2O$$

*4.2.1. Anatase (101).* Two different structures of $V_2O_7H_4$ on the anatase (101) surface were studied. They are shown in Figure 8. The structure in Figure 8a is related to the structure in Figure 2b. In the structure in Figure 8b, the $V_2O_7H_4$ molecule is bound to the surface in such a way that it partially forms the continuation of the anatase crystal structure in the [100] direction. This structure is 63 kJ/mol more stable than the structure in Figure 8a. The adsorption energy is −376 kJ/mol. Vanadium−oxygen bond lengths of this structure are given in Table 3.

A MD simulation at 300 K was performed by starting with the structure in Figure 8b for 10 ps. No noticeable structural distortion occurred within this time scale. But during another MD simulation at 600 K, structural rearrangements were observed within 10 ps similar to those for the monomeric $VO_4H_3$ group on the (101) surface. The V1−O6 and V2−O7 bonds were broken in 5 ps, and the structure shown in Figure 8c was formed. This structure remained stable during the rest of the simulation. Oxygen atoms O1, O2, and O3 were then connected to the 5-fold coordinated titanium atoms on the surface. Their bond lengths are 2.08, 2.08, and 2.28 Å, respectively. Vanadium−oxygen bond lengths and the adsorption energy of this structure are listed in Table 3. The structure in Figure 8c is only 10 kJ/mol more stable than the structure in Figure 8b. This structure is therefore stable at this temperature.

*4.2.2. Anatase (001).* Different adsorption structures of $V_2O_7H_4$ on the (001) surface are shown in Figure 9. In the structure in Figure 9a, the V−V axis in the adsorbate is oriented along the [1$\bar{1}$0] direction. The two vanadium atoms are 5-fold coordinated. In this structure, the dihedral angle between the two V═O groups is 35°. The oxygen O(3) that is bridging the two V atoms is connected to one of the surface titanium atoms. In the case of $VO_4H_3$ adsorption on this surface, the surface oxygen atom bound to vanadium was displaced from its lattice position with the formation of the distorted square-pyramidal structure in Figure 5b. A similar type of adsorption structure was investigated in the case of $V_2O_7H_4$ adsorption, by constructing a model with two oxygens displaced from their lattice positions (structure in Figure 9b) with the formation of two corner-shared distorted square-pyramidal structures. But this possibility is ruled out since a fragmentation of the adsorbate into $VO_5H_2$ and $VO_4H_2$ occurred during the geometry optimization of this structure, and the structure in Figure 9c was obtained.

To investigate the stability of the structure in Figure 9a, a MD simulation at 300 K was performed for 10 ps. During this simulation, the structure in Figure 9a rearranged, and the structure in Figure 9d was obtained. In this structure, the two vanadyl bonds V(1)−O(1) and V(2)−O(2) are connected to two 5-fold coordinated surface titanium atoms, and the two V−OH

**TABLE 3: Adsorption Energies $E_{ads}$ (kJ/mol) and Vanadium−Oxygen Bond Lengths (Å) of Different Adsorbed $V_2O_7H_4$ Structures on the Anatase (101), (001), and (100) Surfaces**

| surface | structure | $E_{ads}$ | bond | bond length |
|---|---|---|---|---|
| (101) | Figure 8b | −376 | V1−O1, V2−O2 | 1.60 |
| | | | V1−O3, V2−O3 | 1.73 |
| | | | V1−O4, V2−O5 | 1.76 |
| | | | V1−O6, V2−O7 | 1.96 |
| | | | V1−O8, V2−O9 | 1.83 |
| (101) | Figure 8c | −386 | V1−O1, V2−O2 | 1.64 |
| | | | V1−O3, V2−O3 | 1.79 |
| | | | V1−O4, V2−O5 | 1.73 |
| | | | V1−O8, V2−O9 | 1.66 |
| (001) | Figure 9d | −439 | V1−O1 | 1.63 |
| | | | V2−O2 | 1.63 |
| | | | V1−O3 | 1.75 |
| | | | V2−O3 | 1.73 |
| | | | V1−O4 | 1.91 |
| | | | V1−O5 | 1.74 |
| | | | V2−O6 | 1.76 |
| | | | V2−O7 | 1.92 |
| | | | V2−O8 | 1.81 |
| | | | V1−O9 | 1.80 |
| (100) | Figure 10a | −315 | V1−O1 | 1.59 |
| | | | V2−O2 | 1.60 |
| | | | V1−O3 | 1.71 |
| | | | V2−O3 | 1.88 |
| | | | V1−O5 | 1.77 |
| | | | V2−O4 | 1.77 |
| | | | V1−O6 | 1.78 |
| | | | V2−O7 | 1.83 |
| | | | V2−O8 | 1.79 |

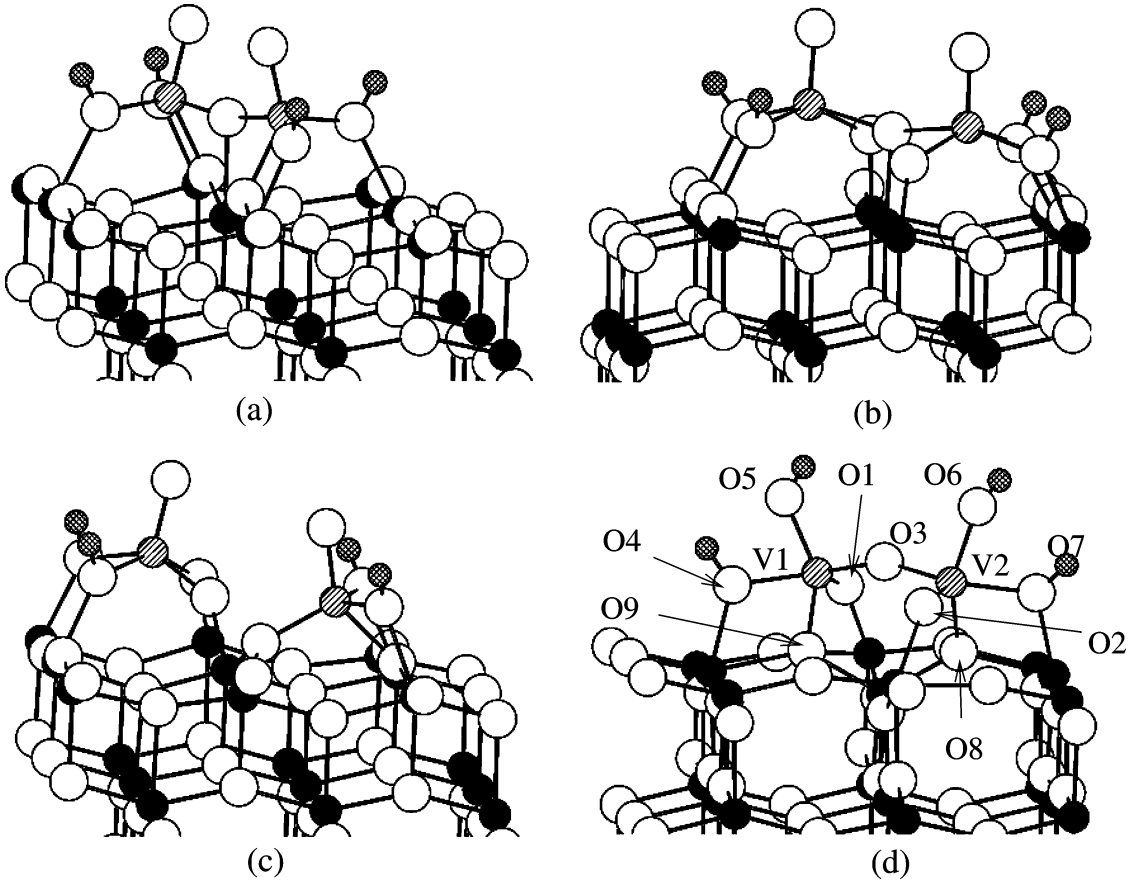


**Figure 9.** Different structures of $V_2O_7H_4$ on the anatase (001) surface. See Figures 1 and 2 for types of atoms.

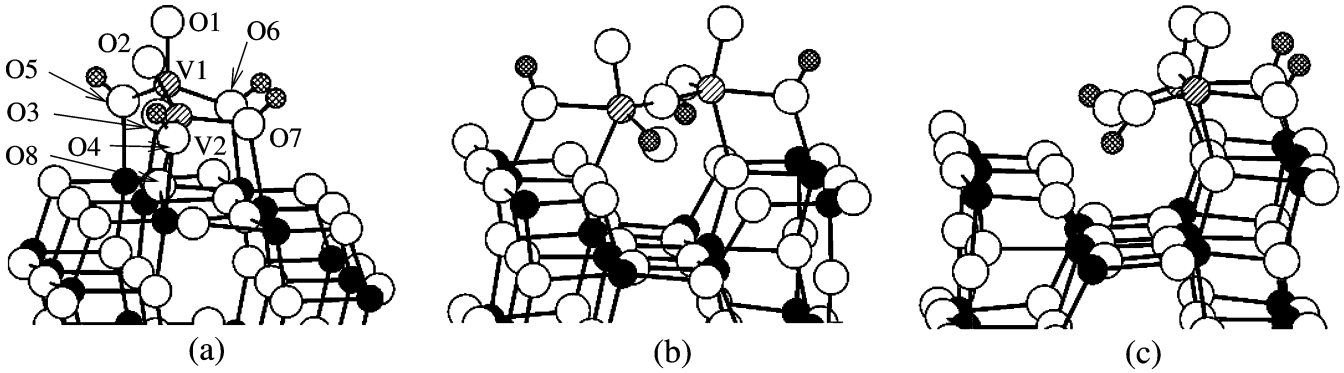


**Figure 10.** Different structures of $V_2O_7H_4$ on the anatase (100) surface. See Figures 1 and 2 for types of atoms.

bonds V(1)−O(5)H and V(2)−O(6)H are pointing upward. Also, the O(3)−Ti bond of the structure in Figure 9a is broken, and consequently the coordination of this oxygen atom changed from three to two. The 5-fold coordinated titanium atom just below this oxygen atom moved downward by approximately 0.4 Å. The whole rearrangement occurred within 2 ps of the simulation. The structure in Figure 9d then remained stable during the rest of the simulation. It is 82 kJ/mol lower in energy than the structure in Figure 9a. This structure was found to be stable in another MD simulation performed at 600 K for 10 ps. The calculated adsorption energy and bond lengths of this structure are given in Table 3.

*4.2.3. Anatase (100).* Three possible adsorption structures of $V_2O_7H_4$ on the (100) surface are shown in Figure 10. In the structure in Figure 10a, the bridging oxygen O(3) in the V−O−V bond is connected to a 5-fold coordinated titanium atom. The two vanadyl bonds V(1)−O(1) and V(2)−O(2) are tilted in opposite directions from the surface normal. Two other possible structures, where $V_2O_7H_4$ is adsorbed at the channels on the (100) surface, were also investigated (Figures 10b and 10c). In the structure in Figure 10b, the $V_2O_7H_4$ is bridging across the channel, while the $V_2O_7H_4$ group is adsorbed on one side of the channel in the structure in Figure 10c. But the structures in Figures 10b and 10c are 71 and 79 kJ/mol, respectively, less stable than the structure in Figure 10a.

Starting from structure in Figure 10a, two MD simulations were performed at 300 and 600 K, respectively, for 10 ps. The structure remained stable during these simulations. The optimized values of the vanadium−oxygen bond lengths of this structure are given in Table 3.

*4.2.4. Discussion.* The most stable structures obtained for the $V_2O_7H_4$ adsorption on the anatase surfaces contain V−O−V bridging groups. $V_2O_7H_4$ partially forms a continuation of the crystal structure along the [100] direction on the anatase (101) surface. This structure undergoes rearrangement, resulting in a structure with 4-fold coordinated vanadium atoms in a tetrahe-

dral environment. In the latter structure, vanadium atoms are connected to oxygen atoms on the surface, and vanadyl groups are absent. In experimental time scale and temperature, both of these structures might coexist. On the anatase (001) surface, no vanadyl groups are present in the adsorbed $VO_x$ species. Similar to the $VO_4H_3$ adsorption, a slightly distorted tetrahedral structure is formed during the adsorption of $V_2O_7H_4$ on the (100) surface. Adsorption at channels on the (100) surface is not favorable.

Raman and IR studies were used to probe the presence of V−O−V bridging groups by their bending bands in the region of 820 $cm^{-1}$.[11,46] The V═O and V−OH groups were also identified by experiments.[12] From the observation of $V_2O_x$ fragments in SIMS experiments, Bond et al.[44] concluded that chains of vanadate groups exist on the $TiO_2$ support. The dimeric vanadates presented in this study are examples of such chains. Went et al.[47] concluded from their Raman spectroscopy studies that polymeric vanadate species have repeating units with divanadyl groups connected by V−O−V bonds. Bulushev et al.[51] proposed a polyvanadate structure with repeating units containing one vanadyl group where vanadium is making one V−O bond in a V−O−Ti arrangement and the vanadyl groups are connected by two V−O bonds via V−O−V. But such structures are not found in the present work. Their interpretation is not conclusive since it cannot be ruled out that the V−O−V arrangement and divanadyl and monovanadyl groups obtained in their experiments belong to different species.

Condensation between $VO_4H_3$ groups can take place under ambient conditions, which could lead to different condensed species such as decavanadate.[14] But such a situation was not considered in the simulations.

We briefly comment on the suitability of the most stable species, i.e., the structures in Figures 8b and 8c on anatase (101), the structure in Figure 9d on anatase (001), and the structure in Figure 10a on anatase (100), for the selective catalytic reduction of $NH_3$ with NO. According to other work,[20,52] V═O groups are necessary. This would exclude the structures in Figures 8c and 9d with two adjacent V−OH groups but not the structures in Figures 8b and 10a with two adjacent V═O groups.

## 5. Summary

Static and dynamic calculations with MSINDO-CCM were used to identify possible structures of hydrated vanadia species on different anatase surfaces. MD simulations have the advantage that the thermal motion of the atoms can be directly described. In this way, free energy barriers can be overcome, and new energy minimum structures can be obtained. $VO_4H_3$ and $V_2O_7H_4$ molecules were adsorbed on the anatase (101), (001), and (100) surfaces, and their stability at 300 and 600 K was studied using constant-temperature MD simulations. The calculations show that vanadia species with divanadyl groups can exist on the anatase (101) surface. In another energy minimum structure of $VO_4H_3$ on this surface, a tetrahedrally coordinated vanadium atom with a vanadium bond to a surface oxygen is present. The adsorption of $VO_4H_3$ results in the formation of an oxygen vacancy on the anatase (001) surface. The vanadate species has a distorted square-pyramidal structure, similar to the $VO_5$ units in the vanadium pentoxide (001) surface. The stable structure of $VO_4H_3$ on the anatase (100) surface consists of a slightly distorted tetrahedron. Adsorption at the channels on the (100) surface was found to be unstable. The most stable structures obtained for the $V_2O_7H_4$ adsorption on the anatase surfaces contain V−O−V units. On the anatase (101) surface, the most stable structure of dimeric hydrated vanadia species contains 4-fold coordinated tetrahedral vanadium centers having vanadium-to-surface oxygen bonds. No vanadyl groups are exposed in this structure. In another possible structure of $V_2O_7H_4$ on the (101) surface, the adsorbate forms a continuation of the anatase crystal structure in the [100] direction. Oxygen vacancies are not created on the (001) surface by the adsorption of a $V_2O_7H_4$ molecule. No vanadyl groups are present in the vanadia species on the anatase (001) surface. A slightly distorted tetrahedral structure is formed during the adsorption of $V_2O_7H_4$ on the (100) surface. Adsorption at the edges or across the channels on the (100) surface is not thermodynamically favorable.

The present investigation shows that different surfaces of anatase are reacting differently with the vanadia particles. The topology of the surface determines the structure of the vanadia species after adsorption. In polycrystalline catalysts, all three anatase (101), (001), and (100) surfaces might be exposed, and corresponding experiments observe an overall effect.

**Acknowledgment.** N. N. Nair gratefully acknowledges a Georg-Lichtenberg fellowship of the state of Niedersachsen. Part of the calculations were performed at the HLRN (Berlin and Hannover), and part of the figures were drawn by SCHAKAL.

## References and Notes

(1) Henrich, V. E.; Cox, P. A. *The Surface Science of Metal Oxides*; Cambridge University Press: Cambridge, 1994.
(2) Henry, J. G.; Heinke, G. W. *Environmental Science and Engineering*; Prentice-Hall: Englewood Cliffs, NJ, 1989.
(3) Nikolov, V.; Klissurski, D.; Anastasov, A. *Catal. Rev.−Sci. Eng.* **1991**, *33*, 319. Matralis, H. K.; Papadopoulou, C.; Kordulis, C.; Elguezabal, A. A.; Corberan, V. C. *Appl. Catal.* **1995**, *126*, 365.
(4) Narayana, K. V.; Venugopal, A.; Rao, K. S. R.; Masthan, S. K.; Rao, V. V.; Rao, P. K. *Appl. Catal., A* **1998**, *167*, 11.
(5) Vejux, A.; Courtine, J. *J. Solid State Chem.* **1978**, *23*, 93.
(6) Lazzeri, M.; Vittadini, A.; Selloni, A. *Phys. Rev. B* **2001**, *63*, 155409.
(7) Beltrán, A.; Sambrano, J. R.; Calatayud, M.; Sensato, F. R.; Andrés, J. *Surf. Sci.* **2001**, *490*, 116.
(8) Oliver, P. M.; Watson, G. W.; Kelsey, E. T.; Parker, S. C. *J. Mater. Chem.* **1997**, *7*, 563.
(9) Bond, G. C.; Tahir, S. F. *Appl. Catal.* **1991**, *71*, 1.
(10) Bond, G. C. *Appl. Catal., A* **1997**, *157*, 91.
(11) Busca, G. *J. Raman Spectrosc.* **2002**, *33*, 348.
(12) Pinaeva, L. G.; Lapina, O. B.; Mastikhin, V. M.; Nosov, A. V.; Balzhinimaev, B. S. *J. Mol. Catal.* **1994**, *88*, 311.
(13) Kozlowski, R.; Pettifer, R. F.; Thomas, J. M. *J. Phys. Chem.* **1983**, *87*, 5176.
(14) Deo, G.; Wachs, I. E. *J. Phys. Chem.* **1991**, *95*, 5889.
(15) Sayle, D. C.; Catlow C. R. A.; Perrin M.-A.; Nortier P. *J. Phys. Chem.* **1996**, *100*, 8940.
(16) Ferreira, M. L.; Volpe, M. *J. Mol. Catal. A: Chem.* **2000**, *164*, 281.
(17) Calatayud M.; Mguig, B.; Minot, C. *Surf. Sci.* **2003**, *526*, 297.
(18) Bredow, T.; Homann, T.; Jug, K. *Res. Chem. Intermed.* **2004**, *30*, 65.
(19) Homann, T.; Bredow, T.; Jug, K. *Surf. Sci.* **2004**, *555*, 135.
(20) Jug, K.; Homann, T.; Bredow, K. *J. Phys. Chem. A* **2004**, *108*, 2966.
(21) Calatayud, M.; Minot, C. *J. Phys. Chem. B* **2004**, *108*, 15679.
(22) Vittadini, A.; Selloni, A. *J. Phys. Chem. B* **2004**, *108*, 7337.
(23) Vittadini, A.; Casarin, M.; Selloni, A. *J. Phys. Chem. B* **2005**, *109*, 1652.
(24) Ahlswede, B.; Jug, K. *J. Comput. Chem.* **1999**, *20*, 563.
(25) Nanda, D. N.; Jug, K. *Theor. Chim. Acta* **1980**, *57*, 95.
(26) Pople, J. A.; Beveridge, D. L.; Dobosh, P. A. *J. Chem. Phys.* **1967**, *47*, 2026.
(27) Zerner, M. C. *Mol. Phys.* **1972**, *23*, 963.
(28) Jug, K.; Geudtner, G.; Homann, T. *J. Comput. Chem.* **2000**, *21*, 974.
(29) Bredow, T.; Geudtner, G.; Jug, K. *J. Comput. Chem.* **2001**, *22*, 861.
(30) Bredow T.; Jug, K. In *Electronic Encyclopedia of Computational Chemistry*; Schleyer, P. von R., Schaefer, H. F., III, Schreiner, P. R., Jorgensen, W. L., Thiel, W., Glen, R. C., Eds.; Wiley: Chichester, U.

K., 2004 (article posted 15 May 2004, http://doi.wiley.com/10.1002/0470845015.cu0001).

(31) Janetzko, F.; Bredow, T.; Jug K. *J. Chem. Phys.* **2002**, *116*, 8994.

(32) Bredow, T.; Geudtner, G.; Jug, K. *J. Comput. Chem.* **2001**, *22*, 89.

(33) Jug, K.; Bredow, T. *J. Comput. Chem.* **2004**, *25*, 1551.

(34) Nair, N. N.; Bredow T.; Jug, K. *J. Comput. Chem.* **2004**, *25*, 1255.

(35) Frenkel, D.; Smit, B. *Understanding Molecular Simulation*; Academic Press: New York, 1996.

(36) Martyna, G. J.; Klein, M. L.; Tuckerman, M. *J. Chem. Phys.* **1992**, *97*, 2635.

(37) Olthoff, B.; Khodakov, A.; Bell, A. T.; Iglesia, E. *J. Phys. Chem. B* **2000**, *104*, 1516.

(38) Chan, S. S.; Wachs, I. E.; Murrel, L. L.; Wang, L.; Hall, W. K. *J. Phys. Chem.* **1984**, *88*, 5831.

(39) Busca, G.; Centi, G.; Marchetti, L.; Trifiró, F. *Langmuir* **1986**, *2*, 568.

(40) Howard, C. J.; Sabine, T. M.; Dickson, F. *Acta Crystallogr., Sect. B: Struct. Sci.* **1991**, *47*, 462.

(41) Hebenstreit, W.; Ruzicky, N.; Herman, G. S.; Gao, Y.; Diebold, U. *Phys. Rev. B* **2000**, *62*, R16334.

(42) Jug, K.; Nair, N. N.; Bredow, T., to be submitted for publication.

(43) Larrubia, M. A.; Busca, G. *Mater. Chem. Phys.* **2001**, *72*, 337.

(44) Bond, G. C.; Vickerman, J. C.; Johnson, D.; Grätzel, M.; Kiwi, J.; Thampi, R.; Albers, P.; Seibold, K. *Catal. Today* **1994**, *20*, 125.

(45) Herrmann, J.-M. *Catal. Today* **1994**, *20*, 135.

(46) Went, G. T.; Leu, L.-J.; Bell, A. T. *J. Catal.* **1992**, *134*, 479.

(47) Went, G. T.; Leu, L.-J.; Lombardo, S. J.; Bell, A. T. *J. Phys. Chem.* **1992**, *96*, 2235.

(48) Machej, T.; Haber, J.; Turek, A. M.; Wachs, I. E. *Appl. Catal.* **1991**, *70*, 115.

(49) Vuurman, M. A.; Wachs, I. E.; Hirt, A. M. *J. Phys. Chem.* **1991**, *95*, 9928.

(50) Fernandez, C.; Guelton, M.; Bodart, Ph.; Rigole, M.; Lefebvre, F. *Catal. Today* **1994**, *20*, 77.

(51) Bulushev, D. A.; Minsker, L. K.; Rainone, F.; Renken, A. *J. Catal.* **2002**, *205*, 115.

(52) Calatayud, M.; Mguig, B.; Minot, C. *Surf. Sci. Rep.* **2004**, *55*, 169.